ELSEVIER

Spectrochimica Acta Part B 54 (1999) 469–480

SPECTROCHIMICA ACTA PART B

Microwave desolvation for acid sample introduction in inductively coupled plasma atomic emission spectrometry

Luis Gras, Juan Mora, José L. Todolí, Antonio Canals*, Vicente Hernandis

Department of Analytical Chemistry, University of Alicante, P.O. Box 99, E-03080 Alicante, Spain

Received 31 July 1997; accepted 14 December 1998

Abstract

This study deals with the behaviour of a microwave desolvation system (MWDS) with acid solutions in inductively coupled plasma atomic emission spectrometry. Hydrochloric, nitric, sulphuric and perchloric acids at different concentrations (up to 0.6 mol l^{-1}) have been tested. Sample uptake rate (Q_l) was also varied. The parameters evaluated for each variable were analyte and solvent transport rates and emission intensity. The combination of low acid concentrations (0.05–0.1 mol l^{-1}) and low liquid flows (0.4 ml min^{-1}) leads to the highest analyte transport rate and emission signal and to the lowest solvent transport rate. For Q_l higher than 1.9 ml min^{-1}, the use of an impact bead is advisable. Among the acids tested, sulphuric and perchloric acids give rise to higher emission intensities than hydrochloric acid and nitric acid. Nonetheless, the limits of detection (LODs) obtained with the MWDS are about the same magnitude irrespective of the solution employed. The LODs reached when using the MWDS are similar to those obtained with a desolvation system based on infrared heating of the aerosol.

Keywords: Microwave desolvation; Aerosol heating; Acid solutions; Inductively coupled plasma atomic emission spectrometry

1. Introduction

Inductively coupled plasma atomic emission spectrometry (ICP-AES) is nowadays one of the most widely used atomic spectrometry techniques in analytical laboratories. This success mainly results from its simplicity, high sample throughput, low limits of detection (LODs) and high dynamic range. Liquid nebulization is the most extensive sample introduction system for routine ICP-AES analysis. In this way, the analyte is introduced into the plasma in the form of an aerosol. The main problem related with this sample introduction technique is the great amount of solvent that is carried to the plasma, together with the analyte. This fact causes a series of interferences (spectral and non-spectral) that are, sometimes, difficult to avoid. The interferent effect of the

* Corresponding author. Tel.: +34-96-5903529; fax: +34-96-5903464; e-mail: antonio.canals@ua.es

0584-8547/99/$ - see front matter
PII: S0584-8547(99)00002-6

solvent in ICP-AES mainly depends on: (i) the amount of solvent transported per unit time (i.e. solvent transport rate, S_{tot}) [1], since low solvent rates can sometimes even show a beneficial influence, whereas high solvent rates are always detrimental; (ii) the physical form in which it is introduced [1], the vapour form being less harmful than the liquid one; (iii) the solvent nature [2–5], organic solvents behaving usually worse than water; (iv) the characteristics of the spectral line [6], since lines for which the excitation energy is lower than the bond energy of the solvent molecule are little influenced, whereas, on the contrary, lines with higher excitation energy are much more affected by the solvent load.

Acidic solutions are very common in the analytical laboratories since they are frequently used for solid sample digestion and solution preservation. Nevertheless, the interferent effect of mineral acids in ICP-AES is well known [7–13]. Acids can make the solvent load to change. Thus, for instance, sulphuric and phosphoric acids cause the mean size of the primary aerosols to increase, thus reducing S_{tot} as well as the analyte transport rate (W_{tot}). Acids can also alter the excitation characteristics of the plasma. Thus, nitric, hydrochloric or perchloric acids do not significantly modify neither the aerosol size nor the solvent load, but they reduce the excitation temperature of the plasma.

Desolvation systems are frequently employed to reduce the solvent load and to increase the analyte transport rate, thus improving sensitivity. Therefore, desolvation systems are very well suited for liquid sample introduction in plasma spectrometers.

During the last years, several applications of microwave (MW) radiation in the field of atomic spectrometry have been suggested: digestion and treatment of solid and liquid samples [14–18], solvent extraction [14,15,19], plasma generation [20], liquid nebulization [21,22], etc. Recently, MW radiation has also been used for aerosol desolvation by means of the so-called microwave desolvation system (MWDS) [23]. The MWDS has been successfully used both in ICP-AES [24] and in inductively coupled plasma mass spectrometry (ICP-MS) [25].

This report is aimed to evaluate the behaviour of the MWDS for acid sample introduction in ICP-AES. To this end, the effect of liquid uptake rate and the nature and concentration of the acid on the solvent and analyte transport rates and on the analytical figures of merit has been studied.

2. Experimental

2.1. Sample introduction system

Fig. 1 shows a scheme of the MWDS setup used in the present work [25]. It includes a pneumatic concentric nebulizer (model AR-35-C2, Glass Expansion Pty. Ltd., Australia) attached to a single-pass spray-chamber (80 cm^3) made of glass. The spray chamber was placed, in a vertical position, at the centre of a domestic MW oven (model W-2235, Balay, Zaragoza, Spain) used as the heating unit, the nominal power of which was 900 W. The MW power was kept constant at its maximum value, i.e. without time chopping. A beaker containing 500 ml of water was placed inside the MW cavity so as to prevent the magnetron from getting damaged, the volume of water being kept constant by means of a peristaltic pump. The nebulizer body was placed outside the cavity with the tip just at the centre of the bottom. Wastes were extracted from the bottom of the spray chamber by means of a peristaltic pump through PTFE tubing. The heating unit was connected through convoluted Gaflon® tubing (25 cm long, 1 cm i.d.) to a condensation unit consisting of two Liebig condensers (33 cm long, 1.2 cm i.d.) coupled in series. The first one was kept at 20°C and the second one at 1°C, so as to reduce the extent of the nucleation processes. A thermostated bath (model F3-K, Haake Mess-Technik GmbH. u. Co., Karlsruhe, Germany) was used to control the temperature of the second condenser.

When the MWDS was used in conjunction with an impact bead, the latter was placed at a distance of 5 mm from the nebulizer tip. Argon was used as nebulizer gas when emission intensity had to be measured, whereas the rest of experiments (i.e. drop size distribution and transport measurements) were done with air. Nebulizer gas flow rate (Q_g) was kept, unless otherwise stated, at 1.0

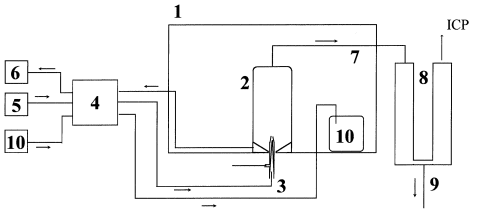

Fig. 1. Experimental setup of the MWDS. (1) Microwave oven; (2) spray chamber; (3) nebulizer; (4) peristaltic pump; (5) sample; (6) spray chamber drain; (7) aerosol conduction; (8) condensation unit; (9) condensation unit drain; (10) water to prevent magnetron damage.

Table 1
Sample introduction system and ICP-AES operating conditions

Sample introduction system	
Nebulizer	Pneumatic concentric AR-35-C2
Sample uptake rate	Variable
Desolvation system	
Condensation temperatures (°C)	
First step	20
Second step	1
Plasma operating conditions	
Gas flow rate (l min^{-1})	
Plasma	16
Auxiliary	1.7
Nebulizer	1.0
Incident power (W)	1200
Reflected power (W)	< 5
Integration time (s)	0.2
Observation height above load coil (mm)	8
PMT gain	4
Torch	Fassel type (4 mm i.d.)

l min^{-1} by means of a calibrated flowmeter (Cole-Parmer Ins. Co., Chicago, IL, USA). Sample uptake rate was varied from 0.4 to 2.4 ml min^{-1} by means of a peristaltic pump (model Minipuls 3, Gilson, Villiers-le-Bel, France). Table 1 summarises the experimental conditions employed.

So as to compare the results obtained with the MWDS, the heating unit of a commercial desolvation system (model Mistral®, Fisons Instruments, Ecublens, Switzerland) based on infrared heating [26] was coupled to the same condensation unit used with the MWDS. This system will be referred to as IRDS from now on. The temperature of the heating unit was 130°C, which is the temperature recommended by the manufacturer for the conditions employed.

2.2. Drop size distribution measurements

Drop size distribution (DSD) of the primary aerosols were measured by means of a laser Fraunhofer diffraction system (model 2600c, Malvern Instruments, Worcestershire, UK). The measurement of the DSD was done at a distance of 5 mm from the nebulizer tip. A lens with a focal length of 63 mm, which enabled the system to measure droplet diameters from 1.2 to 118 μm, was used. The software employed was the B.0D version. A model independent algorithm was used to transform the energy data into DSD. This algorithm does not preclude any particular distribution function. The instrument was previously calibrated by means of a calibration reticule (model IM 062, Malvern Instruments, Worcestershire, UK). The DSD has been characterised by the Sauter median diameter ($D_{3,2}$) and by the fraction of liquid volume contained in droplets smaller than 1.2 μm ($V_{1.2}$).

2.3. Transport measurements

Analyte and solvent transport rates were measured at the exit of the desolvation system using direct methods [24,27]. S_{tot} was determined by nebulizing solutions of Mn (100 μg ml^{-1}), collecting the desolvated aerosol in a U-tube containing dry silica gel and weighing the amount of solvent collected. W_{tot} was measured by nebulizing the same Mn solutions and trapping the exiting aerosol with a glass fibre filter (type A/E, 47 mm diameter, 0.3 μm pore size, Gelman Sciences, Ann Arbor, MI, USA). The filter was then washed out into a volumetric flask with 1.0% (w/w) nitric acid. The analyte content in each volumetric flask

was measured by flame atomic absorption spectrometry.

It was also useful to determine the transport values at the exit of the heating unit. However, the corrosive nature of the aerosols at this point made it difficult to use a direct trapping method to make this measurement. Instead, the aerosol leaving the MW oven (number 7 in Fig. 1) was led to the spray chamber of an atomic absorption spectrometer (model 373, Perkin-Elmer Sciex., Concord, Ontario, Canada), from which the paddles had been previously removed. Under these experimental conditions, absorbance is proportional to W_{tot}, since no drains were observed at the spray chamber of the spectrometer. Therefore, absorbance can be reasonably taken as a sort of determination of W_{tot}, thus making it possible to monitor the trends followed by W_{tot} at the exit of the heating unit.

2.4. ICP-AES instrumentation

Plasma emission intensity was measured with an ICP-AES spectrometer (model 2070, Baird, Bedford, MA, USA). Table 1 shows the instrumental conditions employed. Table 2 lists the elemental lines, wavelengths and spectral bands employed.

LODs were calculated according to the $3s_b$ criterion, s_b meaning the standard deviation from 20 replicates of the blank.

2.5. Reagents

Plain water and solutions of HCl, HNO_3, $HClO_4$ and H_2SO_4 at concentrations ranging from 0.05 to 0.60 mol l^{-1} were used. All chemicals employed were of analytical-reagent grade.

Test solutions containing 1 μg ml^{-1} of each element were prepared by diluting aliquots from a 1000 μg ml^{-1} reference solution (ICP multielemental standard solution IV, Merck, Darmstadt, Germany) in the appropriate solvent.

Table 2
Elements, wavelengths and spectral band width

Element	Wavelength (nm)	Spectral band width (nm)
Zn I	213.856	0.2
Ni II	221.647	0.1
Co II	228.616	0.2
Cd I	228.802	0.1
Mn II	257.610	0.1
Fe II	259.940	0.2
Cr II	283.563	0.2
Cu I	324.754	0.2
Ag I	328.068	0.2

3. Results and discussion

3.1. Transport parameters

3.1.1. Effect of the sample uptake rate

Fig. 2 shows the effect of the sample uptake rate (Q_l) on S_{tot} (Fig. 2A) and W_{tot} (Fig. 2B) at the exit of the desolvation system, for water and for all the acids tested.

Before going to the results, it may be useful to make some comments about what happens and what is expected to occur when Q_l is increased:

1. As it is shown in Table 3, the primary aerosol gets coarser (i.e. its $D_{3,2}$ increases and its $V_{1,2}$ decreases), so that the impaction losses against the inner walls of the spray chamber during the heating step are expected to increase.
2. A larger amount of aerosol is generated.
3. Under the experimental conditions employed in this work, the amount of heat generated by MW absorption is expected to increase, since it is more or less proportional to the amount of liquid introduced into the system.
4. As the argon flow rate is constant, on one hand, and neither argon nor the chamber walls significantly absorb MW radiation by themselves, on the other, heat losses due to argon and chamber walls are expected to become relatively smaller as the amount of sample which is heated by MW absorption is increased.

All these facts have a distinct influence on solvent and analyte transport rates.

Thus, as regards solvent transport rate (Fig. 2A), the impaction losses contribute to the increase in amount of solvent in vapour forming at

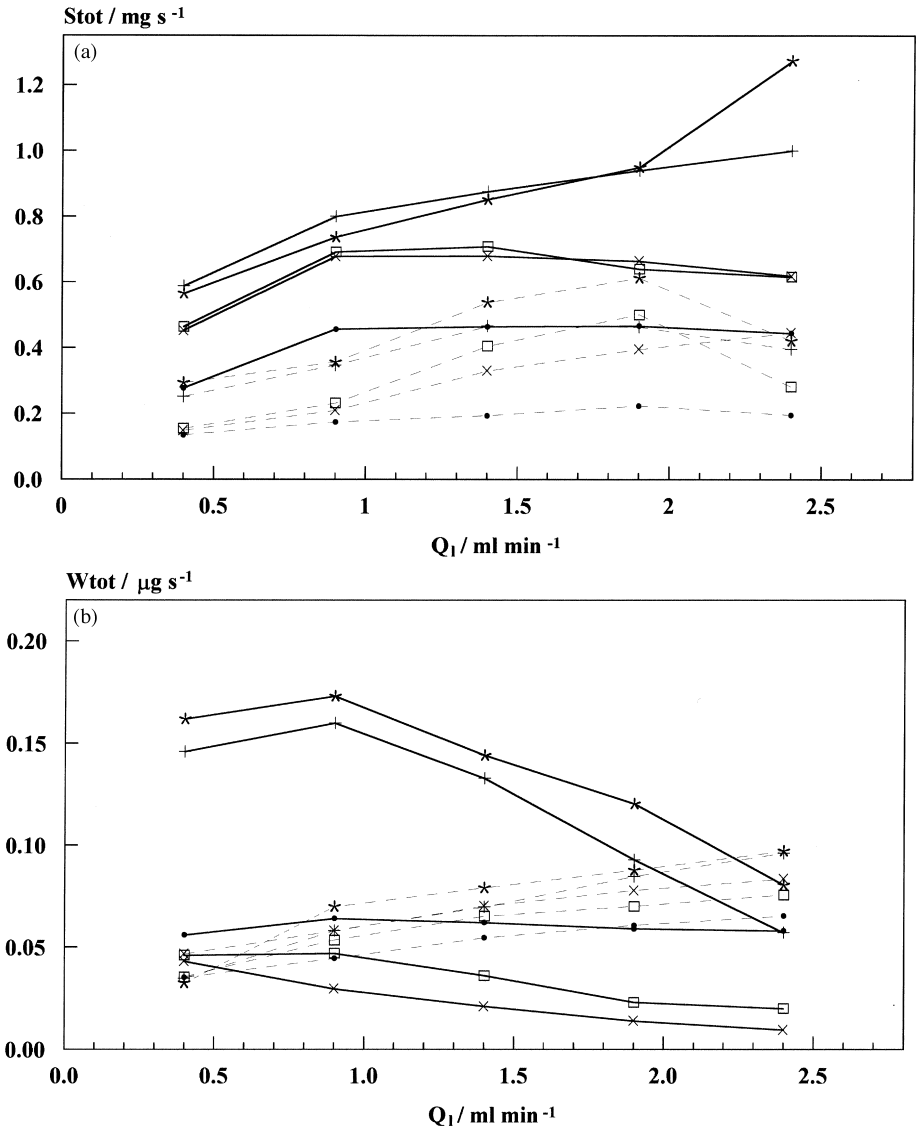

Fig. 2. Effect of the liquid flow rate, Q_l, on (A) the total solvent transport rate, S_{tot}; and (B) the analyte transport rate, W_{tot}, at the exit of the desolvation system for all the solutions studied: (●) water; (×) hydrochloric acid; (□) nitric acid; (+) perchloric acid; and (*) sulphuric acid. Continuous lines: without impact bead; dotted lines: with impact bead. Acid concentration = 0.1 mol l^{-1}; $Q_g = 1.0$ l min^{-1}.

the exit of the heating unit (S_v), as the drops that impact against the walls absorb MW radiation during a long period of time, finally becoming completely vaporised. This fact is confirmed by the very low, or even null, level of drains in the heating unit of the MWDS. On the other hand, factors (2) and (3) cause the amount of solvent evaporated from the droplets surface to increase, thus favouring the transport of solvent in both forms, vapour (S_v) and liquid (S_l). In addition, high values of S_v and S_l at the exit of the heating unit can enhance nucleation in the condensation step [28,29]. The net result of these effects would be an increase in S_{tot} when Q_l is increased (Fig.

Table 3
Drop size distribution of the primary aerosols

Q_l (ml min^{-1})	Concentration (mol l^{-1})	HNO_3		HCl		$HClO_4$		H_2SO_4	
		$D_{3.2}$ (μm)	$V_{1.2}$ (%)	$D_{3.2}$ (μm)	$V_{1.2}$ (%)	$D_{3.2}$ (μm)	$V_{1.2}$ (%)	$D_{3.2}$ (μm)	$V_{1.2}$ (%)
0.4	0.10	5.2	8.7	5.4	8.1	5.5	8.9	5.2	8.4
0.9	0.10	5.5	8.1	5.8	7.9	5.5	8.6	5.5	8.8
1.4	0.10	6.1	7.6	6.2	7.4	5.7	7.4	5.7	7.6
1.9	0.10	6.4	6.9	6.6	7.0	6.4	6.2	6.7	6.1
2.4	0.10	7.3	6.8	7.1	6.9	7.2	5.5	7.7	5.1
0.4	0.00	5.2	8.5	5.2	8.5	5.2	8.8	5.2	8.8
0.4	0.05	5.0	8.3	5.7	8.8	5.1	9.1	5.3	8.3
0.4	0.10	5.2	8.7	5.4	8.1	5.5	8.9	5.2	8.4
0.4	0.20	5.2	8.1	6.0	8.4	5.4	8.8	5.3	8.3
0.4	0.40	5.2	8.1	5.9	8.5	5.6	8.5	5.4	8.2
0.4	0.60	5.3	8.6	5.8	8.5	5.8	7.9	5.0	8.8

2A). This behaviour has been previously observed irrespective of the heating mechanism employed [24,29].

As regards the analyte transport rate, the above mentioned factors (2) and (3) will contribute to enhance W_{tot} when Q_l is increased. Besides, factors (1) and (3) will increase the amount of vapour generated, thus contributing to increase the analyte losses in the spray chamber, due to turbulences, and in the condensation step, due to nucleation [24,28–30]. Fig. 2B (continuous lines) shows two different behaviours of W_{tot} depending on the solution considered. For water, there is no noticeable variation of W_{tot} with Q_l [24], whereas for the acid solutions W_{tot} decreases when Q_l is increased. This decrease might be due to losses

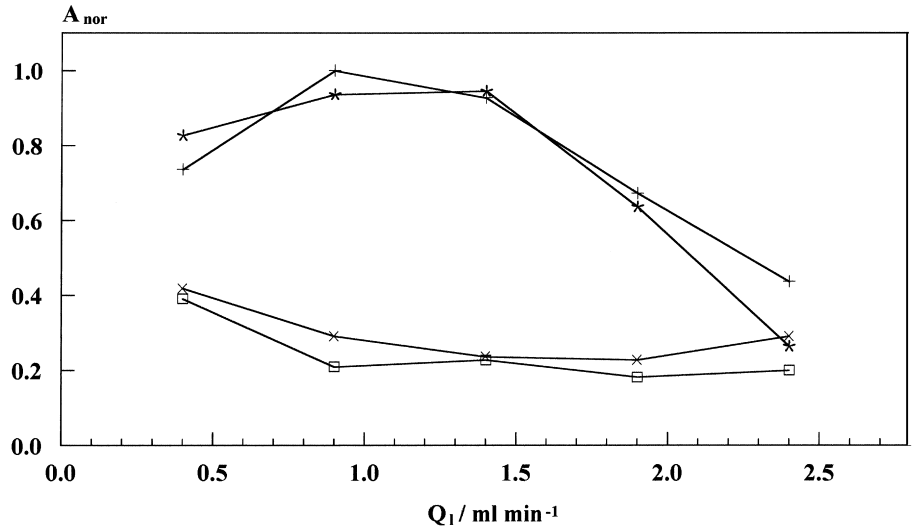

Fig. 3. Effect of the liquid flow rate, Q_l, on the normalised flame atomic absorbance, A_{nor}, obtained at the exit of the heating unit of the MWDS for all the acids studied: (×) hydrochloric acid; (□) nitric acid; (+) perchloric acid; and (*) sulphuric acid. Acid concentration = 0.1 mol l^{-1}; Q_g = 1.0 l min^{-1}.

caused by turbulences in the heating unit and/or by nucleation processes in the condensers. So as to unveil the origin of this decrease, the absorbance at the exit of the heating unit was measured for all the solutions tested, as a means of measuring the relative variations of the analyte transport at this point. The relative absorbance is plotted against Q_l in Fig. 3. It appears that, for all the acid solutions studied, the absorbance decreases when Q_l is increased. This behaviour is similar to that shown in Fig. 2B (continuous lines). This seems to lead to the conclusion that the decrease of W_{tot} upon increasing Q_l observed for the acid solutions can be assigned to analyte losses due to the increasing turbulences inside the heating unit.

In order to reduce the turbulences observed with the MWDS at high sample uptake rates, some experiments have been carried out incorporating an impact bead to the system. The results are shown in Fig. 2 (dotted lines). With the impact bead in place, an up to three times increase in W_{tot} is obtained when Q_l is increased from 0.4 to 2.4 ml min^{-1}. These results can be explained by taking into consideration the effects caused by an impact surface on the characteristics of the aerosol: (i) a reduction of the amount (liquid volume) of aerosol; and (ii) a reduction of the aerosol mean size. Both factors contribute to decrease the amount of aerosol lost by impaction against the walls of the spray chamber during the heating step. In addition, the aerosol lost by impaction against the bead is immediately removed, so that it does not significantly contribute to the vapour generation, thus reducing the analyte losses due to turbulences inside the spray chamber. Therefore, though the introduction of an impact bead gives rise to a reduction in the amount of aerosol generated, this is more than compensated for because of the above mentioned reasons, the final results being a reduction in the amount of solvent vapour generated (i.e. a reduction in S_{tot}, see Fig. 2A) and an increase in W_{tot} when Q_l is increased (Fig. 2B, dotted lines).

3.1.2. Effect of the acid nature and concentration

Fig. 4 shows, for all the acids studied, the effect of the acid concentration on S_{tot} (Fig. 4A) and W_{tot} (Fig. 4B) at the exit of the desolvation system. In general terms, S_{tot} increases on increasing the acid concentration. This result can be explained by taking into account that, for a given solution, the efficiency of MW absorption and, hence, of MW heating, improves when the acid concentration is increased [15]. This represents an increase in S_l since S_v is almost constant (i.e., the aerosol flow is saturated in water vapour at the exit of the condensation step) and an enhancement of the nucleation processes, too.

As regards W_{tot}, Fig. 4B shows two different behaviours. For HCl and HNO_3, there is no significant influence of the acid concentration on W_{tot}. For $HClO_4$ and H_2SO_4, increasing the concentration of the acid solutions causes a steep increase in W_{tot} at the beginning to reach a maximum at concentrations of approximately 0.05–0.1 mol l^{-1} and then a continuous decrease. This last behaviour can be considered as the combined result of two opposite factors: (i) the drop size reduction caused by solvent vaporisation from a droplet's surface, which would contribute to increase W_{tot}; and (ii) the total solvent vaporisation, mainly from the walls of the spray chamber, that would contribute to reduce W_{tot} through turbulence losses and violent vaporisation inside the heating unit and nucleation — gravitational settling losses inside the condensation unit. For a given acid concentration (lower than 0.2 mol l^{-1}), the W_{tot} values obtained for the different acids tested are in the order of $H_2SO_4 > HClO_4 \gg HNO_3 \approx HCl$. Similar relative behaviours have been previously observed in ICP-MS [25]. Since all these solutions show quite similar physical properties (i.e., surface tension, viscosity, density, heat capacity, boiling temperature, etc.), there are no noticeable differences neither among their primary aerosols (see Table 3) nor among their transport capability. Therefore, the differences found between the acid aerosols should be related to their capacity to absorb MW radiation. Pneumatically generated aerosols are composed by charged droplets, the charge of which depends on the nature of the bulk solution from which it is generated [31,32]. MW heating takes place by the interaction between the electrical component of the electromagnetic field and the matter

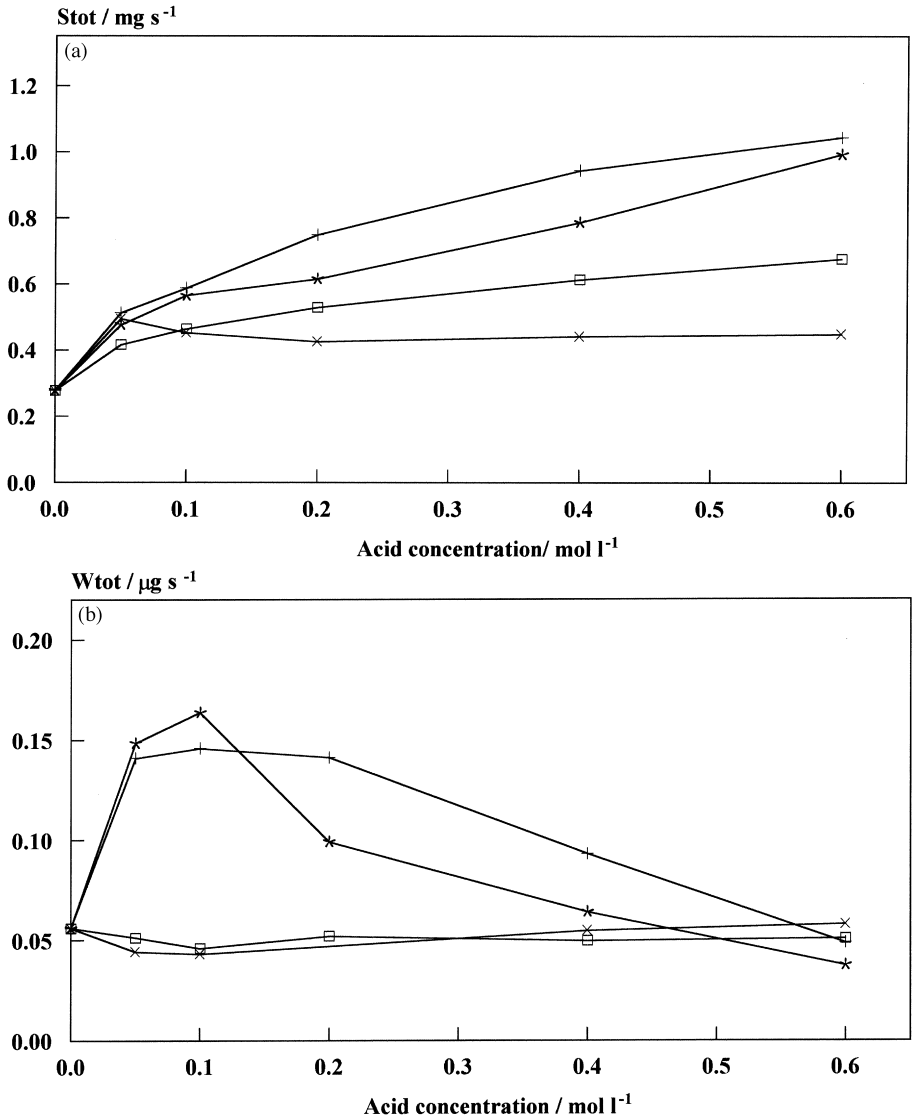

Fig. 4. Effect of the acid concentration on (A) the total solvent transport rate, S_{tot}; and (B) the analyte transport rate, W_{tot}, at the exit of the desolvation system for all the acids tested: (x) hydrochloric acid; (□) nitric acid; (+) perchloric acid; and (*) sulphuric acid. $Q_l = 0.4$ ml min^{-1}; $Q_g = 1.0$ l min^{-1}.

[14,15,33]. Therefore, the differences observed between the aerosols tested might be attributed to their different charge since depending on it, the interaction between the MW field and the matter would be different [25].

From results shown in Fig. 4B, it is clear that H_2SO_4 and $HClO_4$ are heated more efficiently than the remaining acids studied. Among these two acids, turbulences are stronger for sulphuric acid than for perchloric acid, since the former absorbs MW radiation more readily than the second [15,22]. This effect may be invoked to explain why W_{tot} values for H_2SO_4 are lower than for $HClO_4$ at concentrations over 0.1 mol l^{-1}. It is advisable to remember here that the power of the domestic MW oven employed was 900 W. This

value is far too large for our needs, but it was not possible to change it. It seems quite straightforward that the behaviour would have been different using a lower MW power, this is to say, that an increase in the concentration of the acid solution would have caused W_{tot} to increase or, at least, to peak at higher acid concentration values. It is even possible that the nebulization process could be affected by partial solvent vaporisation inside the nebulizer, before its interaction with the gas flow, in spite of the fact that the nebulizer is placed almost entirely out of the MW cavity.

3.2. ICP-AES emission intensity

3.2.1. Effect of the sample uptake rate

Fig. 5 shows the normalised net emission intensity for Mn (I_{nor}) vs. Q_l. The results are in good agreement with what could be expected from the results of W_{tot} and S_{tot} (Fig. 2). Thus, increasing Q_l causes I_{nor} to decrease for the acids, whereas for water it remains unchanged. For the acids, the relative decrease of I_{nor} is more pronounced than that of W_{tot}, due to the increasing value of S_{tot} (Fig. 2A,B). Among the solutions tested, sulphuric acid gives rise to the highest intensities at flow rates below 1.9 ml min^{-1}, whereas water does so at $Q_l \geq 1.9$ ml min^{-1}. This result is consistent with those obtained for the analyte and solvent transport, since at these high liquid flows W_{tot} is only slightly higher for acid solutions than for water (Fig. 2B), whereas S_{tot} is much higher for acid solutions (Fig. 2A).

Fig. 5 (dotted lines) also includes the results obtained for the MWDS with the impact bead in place. As it was observed for W_{tot} (Fig. 2B, dotted lines) the presence of the impact bead modifies the behaviour of I_{nor} with Q_l, causing it to increase in a continuous way. This result is the opposite to that found without the impact bead (Fig. 5, continuous lines). Thus, the emission intensities obtained at 2.4 ml min^{-1} with an impact bead are up to six times higher than without an impact bead.

3.2.2. Effect of the acid nature and concentration

Fig. 6 shows the effect of the acid nature and concentration on I_{nor}. As it was expected from the results shown in Fig. 4, again, two different behaviours can be distinguished. For HCl and HNO_3, the influence of the acid concentration on I_{nor} is very weak. For $HClO_4$ and H_2SO_4, increas-

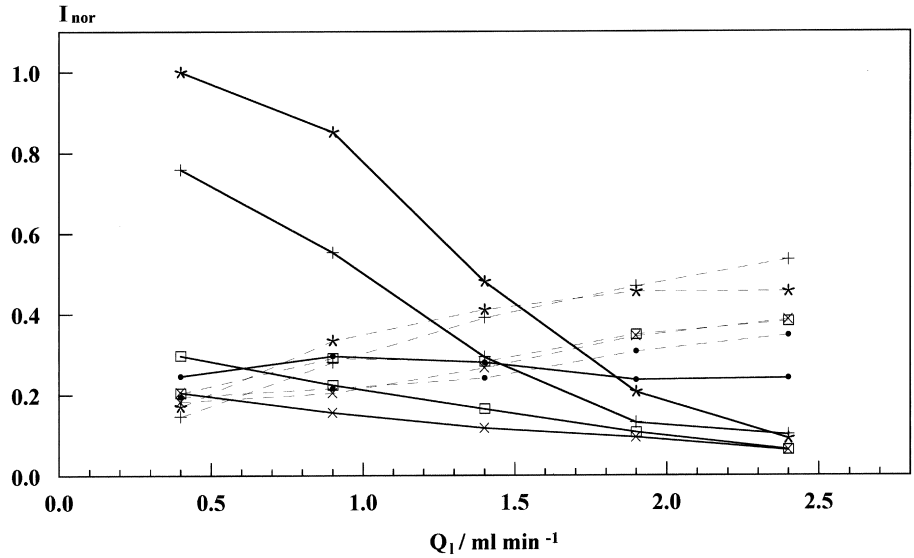

Fig. 5. Effect of the liquid flow rate, Q_l, on the normalised net emission intensity, I_{nor}, for all the solutions studied: (●) water; (x) hydrochloric acid; (□) nitric acid; (+) perchloric acid; (*) sulphuric acid. Continuous lines: without impact bead; dotted lines: with impact bead. Acid concentration = 0.1 mol l^{-1}; Q_g = 1.0 l min^{-1}; [Mn] = 1 μg g^{-1}.

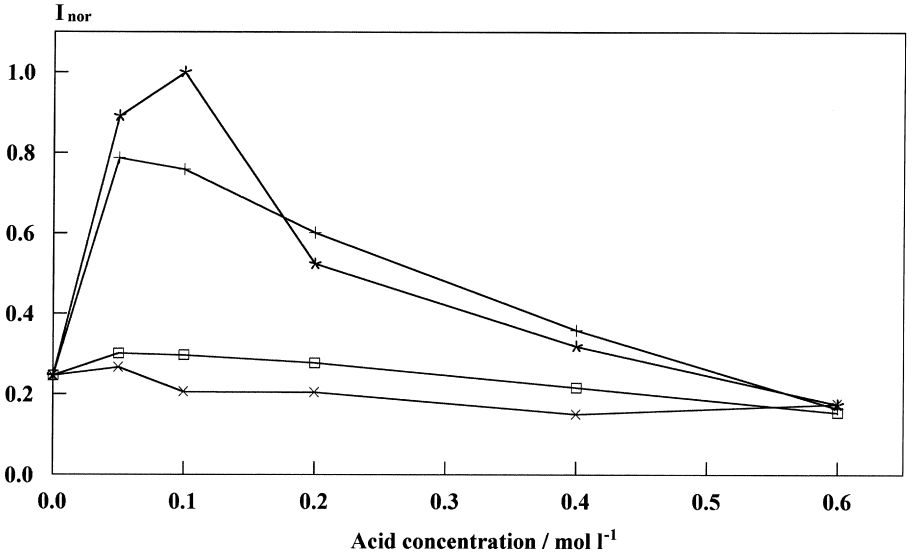

Fig. 6. Effect of the acid concentration on the normalised net emission intensity, I_{nor}, for all the acids tested: (x) hydrochloric acid; (□) nitric acid; (+) perchloric acid; and (*) sulphuric acid. $Q_l = 0.4$ ml min^{-1}; $Q_g = 1.0$ l min^{-1}; [Mn] = 1 μg g^{-1}.

ing the acid concentration causes I_{nor} to reach a maximum at concentrations of 0.05–0.1 mol l^{-1} and then to decrease. At concentrations below 0.2 mol l^{-1}, the I_{nor} values obtained for the different acids tested are, as expected, in the order of $H_2SO_4 > HClO_4 \gg HNO_3 \approx HCl$ [25]. At higher acid concentrations, perchloric acid provides slightly higher intensity than sulphuric acid.

3.3. Limits of detection

Table 4 shows the LODs obtained using the MWDS and the IRDS, without an impact bead, for several elements at 0.4 ml min^{-1}. In these experiments a nebulizer gas flow rate of 0.85 l min^{-1} has been used, since the lowest LODs values are obtained at this value. From the data shown in Table 4 it can be concluded that the LODs obtained with the MWDS are quite similar for the solutions in plain water and sulphuric acid. The results with the remaining acids are also similar. It means that the higher sensitivities obtained with the MWDS for H_2SO_4 and $HClO_4$ compared to those obtained for water, HCl and HNO_3 (Fig. 6) are counterbalanced by the higher level of background noise. On comparing the LODs obtained with the MWDS and the IRDS,

Table 4
Limits of detection (LODs) obtained with the MWDS and IRDS[a]

Element	LODs (ng ml^{-1})			
	Water		Sulfuric acid[b]	
	MWDS	IRDS	MWDS	IRDS
Mn	8	7	11	10
Al	30	30	40	40
Cr	11	9	16	13
Co	10	8	13	11
Fe	4	3	5	4
Mg	12	9	13	13
Cd	4	3	6	5
Ni	18	16	20	20
Zn	6	5	8	7
Ag	12	6	11	8

[a] $Q_l = 0.4$ ml min^{-1}; $Q_g = 0.85$ l min^{-1}.
[b] Acid concentration = 0.1 mol l^{-1}.

Table 4 shows that there are no noticeable differences between both desolvation systems, the results being very close to each other.

4. Conclusions

The best performance of the MWDS is achieved at low sample uptake rates (0.4 ml min^{-1}). For

high sample uptake rates (from 1.9 ml min^{-1}) the use of an impact bead is advisable since it reduces analyte losses in the heating step (due to turbulences) and in the condensation step (due to nucleation).

The behaviour of the MWDS strongly depends on the nature and concentration of the solution used. Thus, microwave heating of the aerosols resulting from the nebulization of acid solutions is, in general terms, more efficient than if no acid is present. This fact gives rise to an improvement in the analyte transport rate and emission intensities. Among the acids tested, sulphuric and perchloric acids give rise to higher signals than hydrochloric and nitric acids do. Using sulphuric or perchloric acids, analyte transport and emission intensities increase with the acid concentration up to 0.1 mol l^{-1}. At higher concentrations, a noticeable decrease in both variables is observed. This behaviour can be accounted for by the turbulences produced by a violent drop vaporisation. Further studies at lower microwave power should be carried out so as to optimise the full process.

The limits of detection obtained with the MWDS are of the same order of magnitude for all acid solutions tested. These LODs are also similar to those obtained with a desolvation system based on infrared heating.

Acknowledgements

The authors thank the DGICyT (Spain) for financial support (Project PB95-0693).

References

[1] S.E. Long, R.F. Browner, The role of water in the inductively coupled argon plasma. Spectrochim. Acta Part B 43 (1988) 1461–1471.

[2] D.G. Weir, M.W. Blades, Characteristics of an inductively coupled plasma operating with organic aerosols. Part 1. Spectral and spatial observations. J. Anal. At. Spectrom. 9 (1994) 1311–1322.

[3] R.I. Botto, J.J. Zhu, Use of an ultrasonic nebulizer with membrane desolvation for analysis of volatile solvents by inductively coupled plasma atomic emission spectrometry. J. Anal. At. Spectrom. 9 (1994) 905–912.

[4] R.I. Botto, J.J. Zhu, Universal calibration for analysis of organic solutions by inductively coupled plasma atomic emission spectrometry. J. Anal. At. Spectrom. 11 (1996) 675–681.

[5] D.R. Wiederin, R.S. Houk, R.K. Winge, A.P. D'Silva, Introduction of organic solvents into inductively coupled plasmas by ultrasonic nebulization with cryogenic desolvation. Anal. Chem. 62 (1990) 1155–1160.

[6] D.E. Nixon, Excitation modulation by water: effects of desolvation on line intensities, temperatures and ion–atom ratios produced by inductively coupled plasmas. J. Anal. At. Spectrom. 5 (1990) 531–536.

[7] M. Marichy, M. Mermet, J.M. Mermet, Some effects of low acid concentrations in inductively coupled plasma atomic emission spectrometry. Spectrochim. Acta Part B 45 (1990) 1195–1201.

[8] J.L. Todolí, J.M. Mermet, Minimization of acid effects at low consumption rates in an axially viewed inductively coupled plasma atomic emission spectrometer by using micronebulizer-based sample introduction systems. J. Anal. At. Spectrom. 13 (1998) 727–734.

[9] A. Fernández, M. Murillo, N. Carrión, J.M. Mermet, Influence of operating conditions on the effects of acids in inductively coupled plasma atomic emission spectrometry. J. Anal. At. Spectrom. 9 (1994) 217–221.

[10] A. Canals, V. Hernandis, J.L. Todolí, R.F. Browner, Fundamental studies on pneumatic generation and aerosol transport in atomic spectrometry: effect of mineral acids on emission intensity in inductively coupled plasma atomic emission spectrometry. Spectrochim. Acta Part B 50 (1995) 305–321.

[11] M. Carré, K. Lebas, M. Marichy, M. Mermet, E. Poussel, J.M. Mermet, Influence of the sample introduction system on acid effects in inductively coupled plasma atomic emission spectrometry. Spectrochim. Acta Part B 50 (1995) 271–283.

[12] J.J. Zhu, Elimination of Acid Matrix and Organic Solvent Interferences in Ultrasonic Nebulization ICP-AES, Pittsburgh Conference, Oral presentation No. 1266, Atlanta, GA, 1993.

[13] X.E. Shen, Q.L. Chen, Effect of a small amount of phosphoric acid in inductively coupled plasma atomic emission spectroscopy. Spectrochim. Acta Part B 38 (1983) 115–121.

[14] A. Zlotorzynski, The application of microwave radiation to analytical environmental chemistry. Crit. Rev. Anal. Chem. 25 (1995) 43–76.

[15] H.M. Kingston, S.L. Haswell (Eds.), Microwave-enhanced Chemistry. Fundamentals, Sample Preparation and Applications, American Chemical Society, Washington, 1997.

[16] A.A. Samra, J.S. Morris, S.R. Koirtyohann, Wet ashing of some biological samples in a microwave oven. Anal. Chem. 47 (1975) 1475–1477.

[17] L. Bordera, V. Hernandis, A. Canals, Automatic flow-injection system for the determination of heavy metals in sewage sludge by microwave digestion and detection by inductively coupled plasma-atomic emission spectrometry (MW-ICP/AES). Fresenius J. Anal. Chem. 355 (1996) 112–119.

[18] A. Cuesta, J.L. Todolí, J. Mora, A. Canals, Rapid determination of chemical oxygen demand by a semi-automated method based on microwave sample digestion, chromium(VI) organic solvent extraction and flame atomic absorption spectrometry. Anal. Chim. Acta 372 (1998) 359–369.

[19] J.R.J. Paré, J.M.R. Belanger, S.S. Stafford, Microwave-assisted process (MAP^{TM}): a new tool for the analytical laboratory. Trends Anal. Chem. 13 (1994) 176–184.

[20] J.F. Camuña-Aguilar, R. Pereiro-Garcia, J.E. Sanchez-Uría, A. Sanz-Medel, A comparative study of three microwaves-induced plasma sources for atomic emission spectrometry — II. Evaluation of their atomization/excitation capabilities for chlorinated hydrocarbons. Spectrochim. Acta Part B 49 (1994) 545–554.

[21] L. Bordera, J.L. Todolí, J. Mora, A. Canals, V. Hernandis, Characterization of the aerosols generated by a new microwave thermal nebulizer. J. Aerosol Sci. 27 (1996) S387–S388.

[22] L. Bordera, J.L. Todolí, J. Mora, A. Canals, V. Hernandis, A microwave-powered thermospray nebulizer for liquid sample introduction in inductively coupled plasma atomic emission spectrometry. Anal. Chem. 69 (1997) 3578–3586.

[23] V. Hemandis, A. Canals, J. Mora, L. Gras, Sistema de Desolvatación por Microondas para uso en Espectrometría Atómica, Patent number P9500810, Spain, 1995.

[24] L. Gras, J. Mora, J.L. Todolí, A. Canals, V. Hernandis, Behaviour of a desolvation system based on microwave radiation heating for use in inductively coupled plasma atomic emission spectrometry. Spectrochim. Acta Part B 52 (1997) 1201–1213.

[25] J. Mora, A. Canals, V. Hernandis, E.H. van Veen, M.T.C. de Loos-Vollebregt, Evaluation of a microwave desolvation system in inductively coupled plasma mass spectrometry with low acid concentration solutions. J. Anal. At. Spectrom. 13 (1998) 175–181.

[26] A. Eastgate, W. Vogel. Sample Nebulizer and Evaporation Chamber for ICP and MIP Emission or Mass Spectrometry and Spectrometers Comprising the Same, Patent Number 5,534,998, USA, 1996.

[27] J. Mora, J.L. Todolí, A. Canals, V. Hernandis, Comparative studies of several nebulizers in inductively coupled plasma atomic emission spectrometry: low pressure versus high pressure nebulization. J. Anal. At. Spectrom. 12 (1997) 445–451.

[28] W.C. Hinds, Aerosol Technology: Properties, Behaviour and Measurement of Airborne Particles, John Wiley and Sons, New York, 1982.

[29] J. Mora, J.L. Todolí, I. Rico, A. Canals, Aerosol desolvation studies with a thermospray nebulizer coupled to inductively coupled plasma atomic emission spectrometry. Analyst 123 (1998) 1229–1234.

[30] M.A. Tarr, G. Zhu, R.F. Browner, Transport effects with dribble and jet ultrasonic nebulizers. J. Anal. At. Spectrom. 7 (1992) 813–817.

[31] L.B. Loeb, Static Electrification, Springer-Verlag, Berlin, 1958.

[32] M.J. Matteson, The separation of charge at the gas–liquid interface by dispersion of various electrolyte solutions. J. Colloid Interface Sci. 37 (1971) 879–890.

[33] A. Canals, L. Gras, J. Mora et al., Insight into the interaction of the microwave radiation with droplets of interest in analytical chemistry, Spectrochim. Acta Part B, 54 (1999) 333–342.